minerals

MDPI

Article

Predicting the Risk of Fault-Induced Water Inrush Using the Adaptive Neuro-Fuzzy Inference System

Qinglong Zhou *, Juan Herrera-Herbert and Arturo Hidalgo

Departamento de Ingeniería Geológica y Minera, ETS de Ingenieros de Minas y Energía, Universidad Politécnica de Madrid (UPM), C/Alenza 4, 28003 Madrid, Spain; juan.herrera@upm.es (J.H.-H.); arturo.hidalgo@upm.es (A.H.)

* Correspondence: zhou198773@gmail.com

Academic Editor: Saiied Aminossadati

Received: 4 February 2017; Accepted: 5 April 2017; Published: 7 April 2017

Abstract: Sudden water inrush has been a deadly killer in underground engineering for decades. Currently, especially in developing countries, frequent water inrush accidents still kill a large number of miners every year. In this study, an approach for predicting the probability of fault-induced water inrush in underground engineering using the adaptive neuro-fuzzy inference system (ANFIS) was developed. Six parameters related to the aquifer, the water-resisting properties of the aquifuge and the mining-induced stresses were extracted as the major parameters to construct the ANFIS model. The constructed ANFIS was trained with twenty reported real fault-induced water inrush cases, and another five new cases were used to test the prediction performance of the trained ANFIS. The final results showed that the prediction results of the five cases were completely consistent with the actual situations. This indicates that the ANFIS is highly accurate in the prediction of fault-induced water inrush and suggests that quantitative assessment of fault-induced water inrush using the ANFIS is possible.

Keywords: water inrush; fuzzy neural network; mining engineering; ANFIS

1. Introduction

In mining activities, unexpected volumes of groundwater that rush into a working face or a heading face in a short period of time can be a fatal disaster, killing miners and flooding equipment. Currently, water inrushes still occur all over the world, especially in coal producing countries such as United States, Australia, China, Poland and India [1–4]. Frequent water accidents, on the one hand, seriously affect miners' safety and on the other hand affect productivity. Predicting the probability of a water inrush accurately and then taking some effective countermeasures before mining or excavating therefore becomes an important and urgent issue for the safety management of underground mining engineering.

The frequent occurrence of water inrush accidents can be attributed, in part, to the geological complexity and stress complexity of underground mining, but we must admit that it is also due to our underdeveloped water inrush risk assessment system. Taking China as an example, an underdeveloped empirical formula proposed in the 1960s [5] is still applied today to assess the inrush risk throughout the country.

In recent years, soft computing techniques such as artificial neural networks (ANN), fuzzy inference system (FIS) and adaptive neuro-fuzzy inference system (ANFIS) have already provided solutions for a wide range of engineering problems [6–19]. However, for the water inrush problem in underground engineering, there are still only a few studies [4,20] in this field.

In this study, our aim is to apply the ANFIS (the combination of the ANN and FIS) to predict the probability of water inrush. This study is organized as follows. In the next section, a brief

description of the mechanisms and major influencing factors of the fault-induced water inrush will be given. The algorithm of the ANFIS will be given in Section 3; and the training, testing and prediction performances of the ANFIS will be given in Section 4.

2. Brief Description of Fault-Induced Water Inrush

2.1. Water-Conducting Property of Fault

In most cases, the main reason for fault-induced water inrush is that the fault itself has a good water-conducting property. This property is mainly determined by two aspects. First, hydro-mechanical units within the fault zone are generally high permeability structures [21–26]; the typical structural elements of a fault zone are given in Figure 1. Second, besides the feature of high permeability, the fault zone itself is a water-bearing structure filled with fluid, especially when it is connected to an aquifer [27].

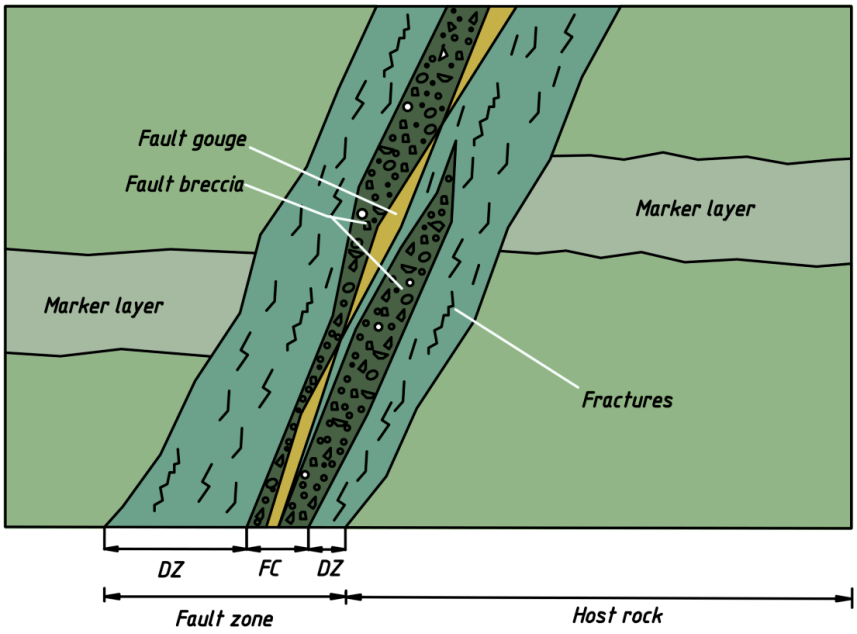

Figure 1. Typical structural elements of a fault zone. Generally, it consists of two parts: damage zone (DZ) and fault core (FC); fault gouge and fault breccia are structure elements within the fault core and sets of fractures are subsidiary structures in damage zones. Modified from Gudmundsson [23].

2.2. Brief Introduction to Fault-Induced Water Inrush

In some cases, a coal seam and an aquifer can be cut simultaneously by a large fault (see Figure 2), and a fault generally acts as a water-conducting structure, thus directly connecting the aquifer and the coal seam. In this case, a water inrush accident may occur suddenly when a working face is close to the fault.

A small fault can also lead to water inrush accidents (Figure 3). In most cases, small faults are not connected with a coal seam, however under the coupling actions of mining-induced stresses and hydraulic pressure, the fault reactivation [27–31] can occur and therefore form a water inrush passageway. On the one hand, whether or not a fault reactivation occurs is related to the fault-tip stress concentration scale caused by mining-induced stresses, and on the other hand is related to the relative position between the fault and the working face. As for the fractured water-conducting zone in the floor caused by mining-induced stresses, according to Li's work [32], by conducting a correlation

analysis between the related mining parameters and the size of the fractured zone in 16 working faces, he came to the following regression formula:

$$h = 0.0175H + 0.1463\alpha + 3.3817M + 0.0508L - 7.76695 \quad (1)$$

where h is the depth of the water-conducting fractured zone; H is the mining depth; α is the dip angle of the coal seam; M is the mining height; L is the length of the working face. As can be seen from this formula, the correlation coefficient of the mining height is the largest, which means that the mining height has the most significant influence on the size of the fractured zone, followed by the dip angle of the coal seam; more investigations about how the fractured zone is affected by the dip angle of the coal seam can also be seen from Miao and Zhang's works [3,33].

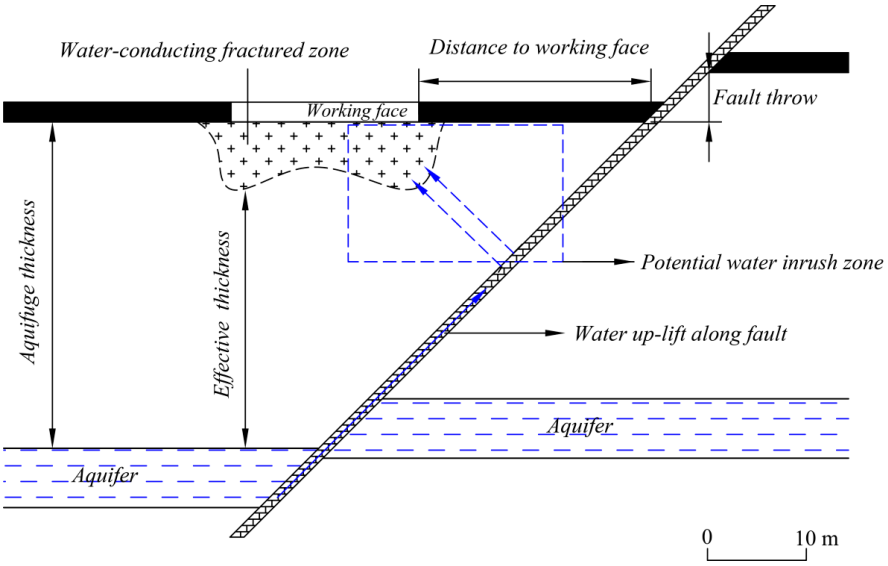

Figure 2. The coal seam and the aquifer are connected by a large fault.

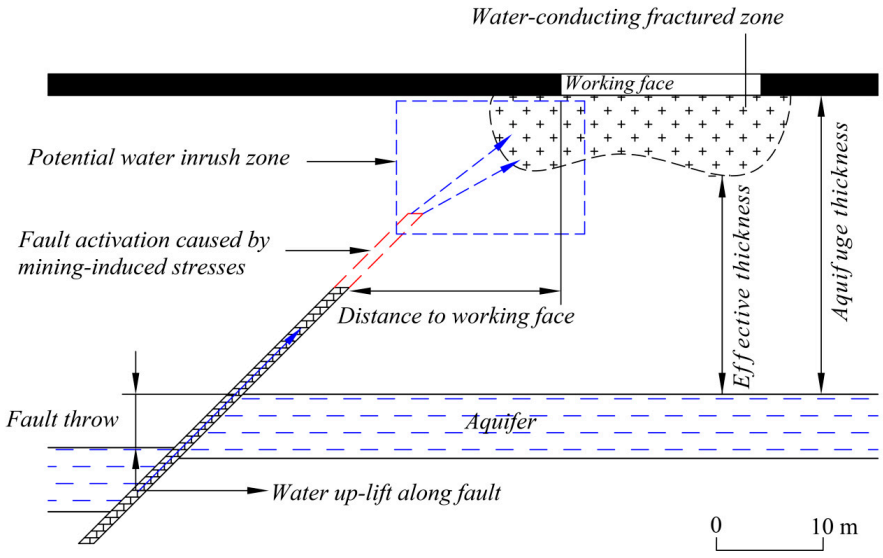

Figure 3. A small fault is connected to an aquifer but not to a coal seam.

In the process of mining, a water-conducting fault mainly affects water inrush in the following aspects. Groundwater in the aquifer can be raised to a certain height by the water-conducting fault,

thus reducing the effective thickness of the aquifuge. In some cases, groundwater may even be directly raised to a coal seam with the aquifuge completely losing its water-resisting function. Sometimes, a large fault may cut through multiple aquifers and these cut aquifers are thus hydraulically linked. If water inrush occurs in such a case, then there will be a large volume of groundwater related.

3. Methodology of the ANFIS

Based on fuzzy theory and fuzzy logic inference, the FIS has the advantage of simulating the reasoning process of the human brain [34] and has the advantage of solving problems that are described in the language of uncertainty. The ANN simulates the working mechanisms of the human brain from another perspective [35,36]. It is structured by a number of interconnected processing artificial neurons, therefore it can mimic the human brain to process data in parallel.

The ANFIS combines the advantages of the ANN and FIS. It uses the self-learning process of the ANN to process data in parallel and to realize automatic fuzzy inference. In the ANFIS, the input and output nodes of the neural network are used to express the input and output signals of fuzzy systems, and the membership functions and fuzzy rules of fuzzy systems are represented by the hidden notes of the neural network.

3.1. Architecture of ANFIS

As an example, Figure 4 shows a typical ANFIS model [37,38] with two inputs, x and y, and an output, f, for the first-order Sugemo fuzzy model [39]. Two rules were employed:

$$Rule^1 \ : if\ x\ is\ A_1\ and\ y\ is\ B_1,\ then\ f_1 = p_1x + q_1y + r_1$$

$$Rule^n \ : if\ x\ is\ A_2\ and\ y\ is\ B_2,\ then\ f_2 = p_2x + q_2y + r_2$$

As can be seen, in these two rules the input part is fuzzy but the output part is a certain linear function (sometimes it could also be a constant), and A_1, B_1, A_2, B_2 represent the membership functions for x and y; p_1, q_1, r_1, p_2, q_2, r_2, are the parameters for all the fuzzy systems.

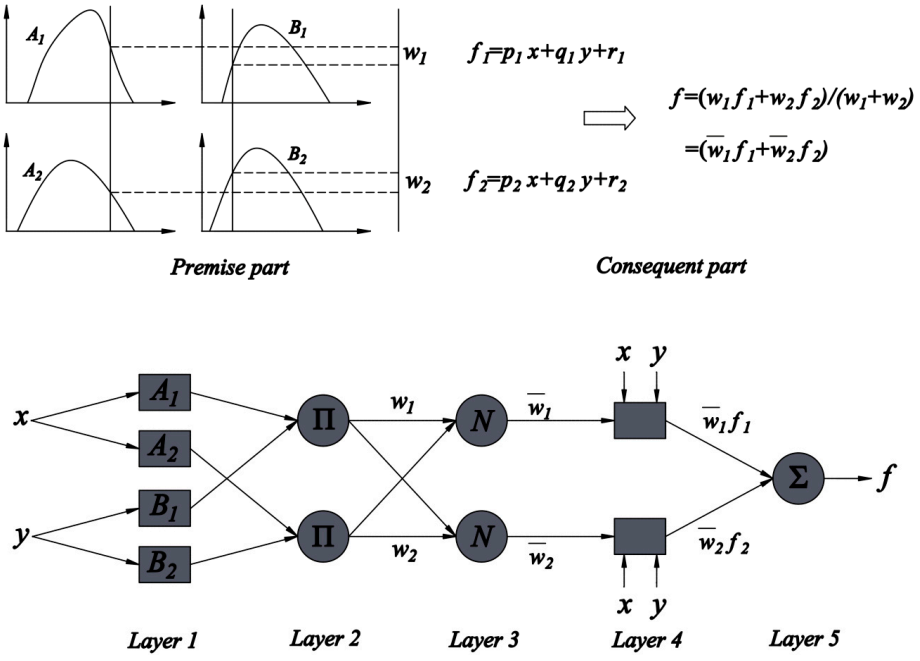

Figure 4. A typical adaptive neuro-fuzzy inference system (ANFIS) model with two inputs and one output.

The process of fuzzy reason is illustrated in Figure 4 [38,39]; as can be seen from the figure, an ANFIS consists of five layers [37]. Layers marked by squares are adaptive layers, which means that their node values are adjustable. On the contrary, layers marked with circles have fixed parameter sets.

Layer 1: The first layer of this system is the fuzzy layer, and each node of this layer is an adaptive node and represents a fuzzy linguistic variable. If we choose a Gaussian function as the membership function, then the membership grade of every element of the inputs could be calculated as follows:

$$O_{1,i} = \mu_{A_i}(x) = (\exp(-(x - c_i))^2/\sigma_i) \ (i = 1, 2) \tag{2}$$

$$O_{1,i} = \mu_{B_i}(y) = (\exp(-(y - c_i))^2/\sigma_i) \ (i = 1, 2) \tag{3}$$

where c_j and σ_j are two premise parameters that could change the shape of the membership function while c_j denotes the center of the membership function and σ_j represents its width.

Layer 2: Labeled as Π, each node of layer 2 is a fixed node which is represented by a circle, and the output of each node is calculated by means of the 'product' of all the incoming signals of the first layer:

$$O_{2,i} = w_i = \mu_{A_i}(x) u_{B_i}(y) \ (i = 1, 2) \tag{4}$$

The output w_i is the firing strength of the corresponding rule.

Layer 3: Each node of this layer is also a fixed node marked with a circle and labeled as N, denoting the normalized firing strengths of every rule. The outputs for this layer are computed by using Equation (5) as:

$$O_{3,i} = \overline{w}_i = w_i / (w_1 + w_2) \ (i = 1, 2) \tag{5}$$

where $\overline{w}_i$ is the normalized firing strength.

Layer 4: For this layer, every node represents a node function (see Equation (6)), and each adaptive node of this layer represents the contribution of the i-th rule to the overall output.

$$O_{4,i} = \overline{w}_i f_i = w_i(p_i x + q_i y + r_i) \ (i = 1, 2) \tag{6}$$

Corresponding to the above mentioned premise parameters, here p_i, q_i, r_i are called the consequent parameters.

Layer 5: In this layer, the overall outputs, which are the sum of all incoming signals of the previous layers, are calculated through the sum operation (Σ):

$$O_{5,i} = f = \sum_i \overline{w}_i f_i = \frac{\sum_i (w_i f_i)}{\sum_i w_i} \ (i = 1, 2) \tag{7}$$

3.2. Hybrid Learning Rule of the ANFIS

The learning process of the ANFIS is actually a process of learning knowledge from the training samples by adjusting the premise parameters and the consequent parameters, which is achieved by using the gradient method and the least squares method [40,41]. For the above described ANFIS model, if we rewrite Equation (7) as Equation (8), clearly we can see from Equation (8) that the overall output of the model can be expressed as a linear combination of the consequent parameters. Supposing t is the target value and f is the actual output, the aim of the learning process is actually to find the optimal consequent parameters that could minimize the error function e between t and f (see Equation (9)).

$$f = \sum_i \overline{w}_i f_i = (\overline{w}_1 x)p_1 + (\overline{w}_1 y)q_1 + (\overline{w}_1)r_1 + (\overline{w}_2 x)p_2 + (\overline{w}_2 y)q_2 + (\overline{w}_2)r_2 \tag{8}$$

$$e = (f - t)^2 \tag{9}$$

As discussed in Jang's research [42], the learning process includes a forward pass and a backward pass. In the forward pass, the functional signals go forward until layer 4 and the consequent parameters (in layer 4) are identified by the least squares estimate; whereas in the backward pass, the error rate propagates backward and the premise parameters are updated by the gradient decent.

4. Prediction of Fault-Induced Water Inrush with the ANFIS

As discussed in Section 2, fault-induced water inrushes are affected by multiple factors and each of them has a different role in water inrushes. The aquifer pressure is the most important factor since it always acts as a dynamic factor to trigger an inrush accident. The fault, which is like a bridge that connects the aquifer and the seam, often acts as a conduit to allow water flow from an aquifer to a coal seam. The aquifuge, on the contrary, has a restraining role to resist water flow from an aquifer to a coal seam.

Corresponding to the above mentioned factors, water pressure (WP); distance to working face (DWF) (detailed representation can be seen in Figures 2 and 3); fault throw (FT); mining height (MH); dip angle of coal seam (DACS); and aquifuge thickness (AT) are therefore introduced as the six main parameters to predict water inrush in this study. Here, the WP is used for representing the hydraulic property of the aquifer; the DWF and the FT are used for indicating the relative position between the fault and the working face; the size of the mining-induced fractured zone is mainly determined by the MH and DACS; and we use AT to indicate the water-resisting capability of the aquifuge.

4.1. ANFIS Training

To train the ANFIS, the first step is the determination of the input parameters and the desired output. The six main parameters mentioned above are selected as the input parameters. If we use 1 and -1 (named as the water inrush index) to represent water inrush occurring and not occurring respectively, then 1 and -1 can be used as the numerical desired outputs to implement ANFIS training. The ANFIS structure implemented is illustrated in Figure 5 with input and output parameters.

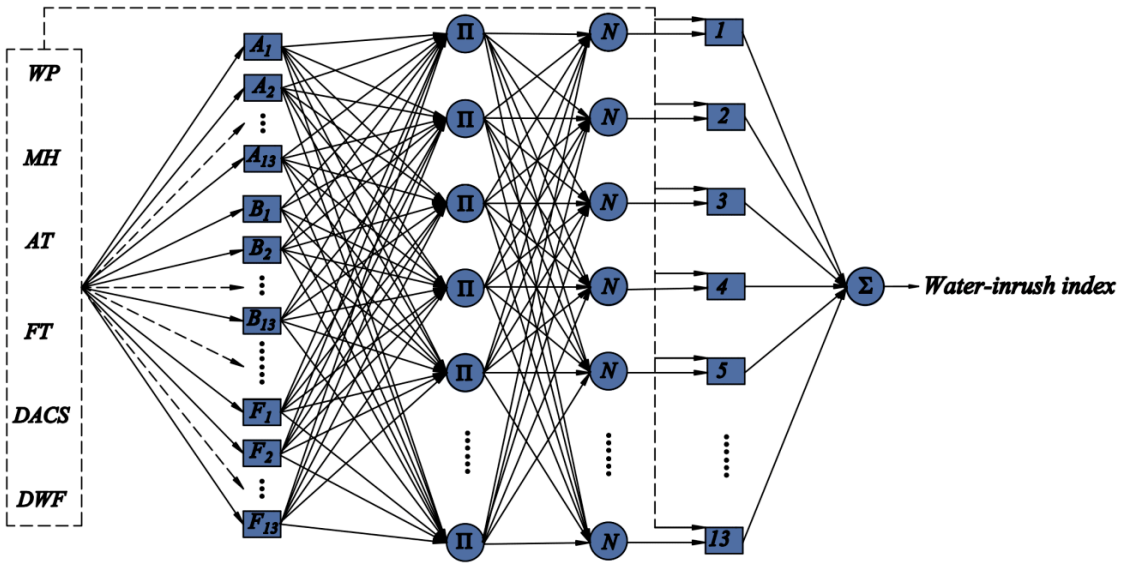

Figure 5. ANFIS structure used for the assessment of the water inrush index.

For the ANFIS, its prediction is based on the training and learning from known samples. Hence, in this work, real water inrush cases reported by Shi [43] were selected as training samples (see Table 1).

Table 1. Real water inrush cases used for ANFIS training (reported by Shi [43]).

Mines	(WP)/MPa	(MH)/m	(AT)/m	(FT)/m	(DACS)/°	(DWF)/m	Whether Water Inrush Accident Occurred in Actual Situation?
Xiazhuang coal mine case 1	1.82	0.8	26.39	4	12	16	Yes
Xiazhuang coal mine case 2	1.65	1.6	25.85	50	17	90	Yes
Xiazhuang coal mine case 3	1	0.9	22.33	2	13	16	Yes
Xiazhuang coal mine case 4	2.88	1	17.68	1.3	20	0	Yes
Jingxing coal mine case 1	2.01	8	28	0.6	18	10	Yes
Jingxing coal mine case 2	1.91	8	43	1.5	11	2	Yes
Hongshan coal mine case 1	1.33	0.85	36.38	0.8	7	62	No
Hongshan coal mine case 2	0.95	1.45	26.89	1	6	55	No
Hongshan coal mine case 3	0.92	1.4	33.61	0.5	8	0	No
Hongshan coal mine case 4	0.34	0.9	32.65	22	6	6	No
Heishan coal mine case 1	1.06	2	27.79	0.46	7	21	No
Heishan coal mine case 2	0.83	2.85	26.56	0.7	12	6	No
Xieyi coal mine	2	2.81	30	1.5	18	12	Yes
Jiulishan coal mine	1.87	1.9	23	0.5	15	17	Yes
Pandong coal mine	1.7	2.8	10	5	17	10	Yes
Taoyang coal mine	0.6	1.1	17	8	19	6	Yes
Huatai coal mine	2.1	1.6	59.5	3.5	10	39	No
Panxi coal mine case 1	2.8	2.75	69.17	11.7	12	36	No
Panxi coal mine case 2	2.8	2.55	66.11	16	12	29	No
Xiezhuang coal mine	1.3	1.7	30	4.9	5	21	Yes

WP: water pressure; MH: mining height; AT: aquifuge thickness; FT: fault throw; DACS: dip angle of coal seam; DWF: distance to working face.

Before starting the training process, first of all, the initial FIS needs to be generated. The key to this step is to determine the number of membership functions for each of the corresponding input parameters, and the shape of the membership functions of the premise part. For the shape of the membership functions, in this study, Gaussian shaped membership function was selected. In general, the grid partition and subtractive clustering are the two ways which have been widely applied for generating the initial FIS. By setting all initial water inrush indexes as 0 and by choosing the subtractive clustering approach to generate the initial FIS, 13 *if-then* rules were thereby generated as can be seen in Figure 6A. The advantage of the subtractive clustering technique is that a large data set can be automatically distilled into several natural groups, thus resulting in a concise representation of a system's behavior [44]. A more detailed description of the subtractive clustering technique can be seen in Chiu's further work [45]. In this study, for generating the initial FIS, the corresponding system parameter values are set as follows: range of influence is 0.65, squash factor is 1.25, acceptance ratio is 0.5 and rejection ratio is 0.15.

The ANFIS was trained by using the hybrid training algorithm as described in Section 3.1. The shapes of the membership functions, which are determined by the initial FIS rules, were constantly adjusted by the ANFIS training process. In this study, after 18 epochs of training, the training accuracy meets the requirements, and the outputs of the ANFIS were exactly consistent with the desired outputs (see Figure 7). After the training process, the 13 initial FIS rules were modified as can been seen in Figure 6B, and the final shapes of the membership functions correspond to the six main parameters, as shown in Figures 8 and 9.

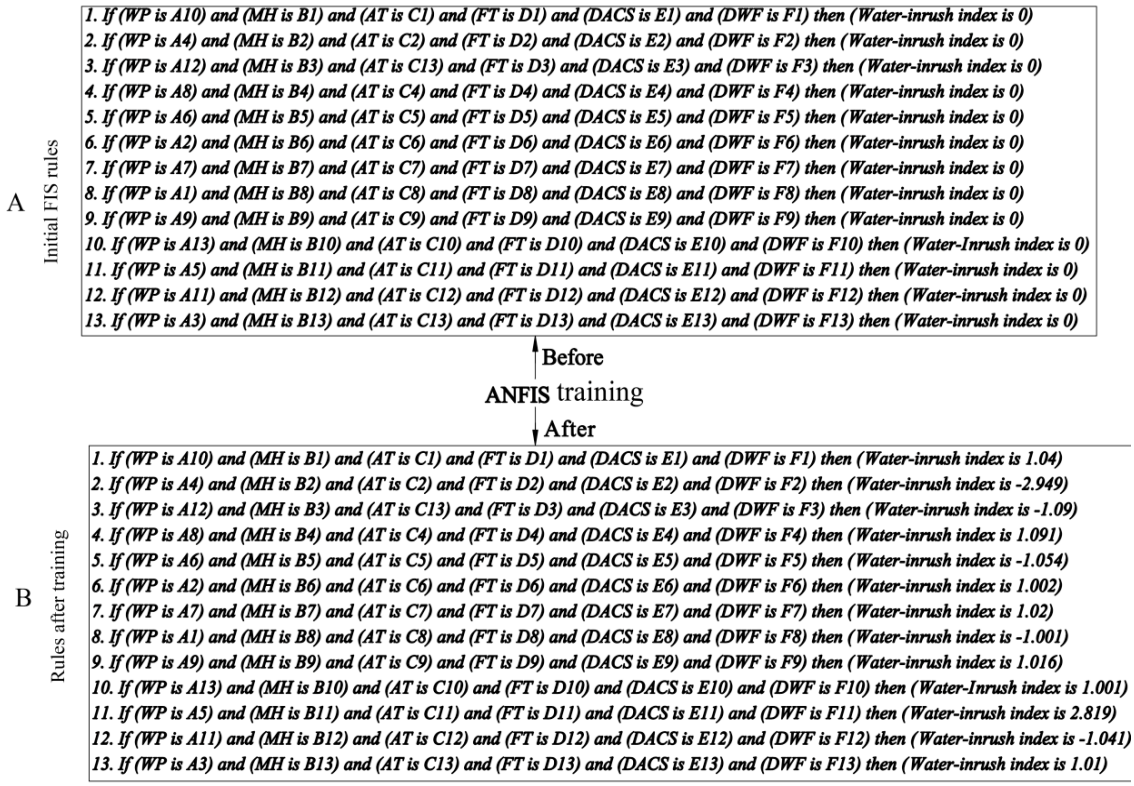

Figure 6. The initial fuzzy inference system (FIS) rules before training and after training. In this figure: (**A**) refers to the 13 initial FIS rules which are generated by using the subtractive clustering approach and (**B**) refers to the 13 trained FIS rules which are obtained by using the hybrid training algorithm.

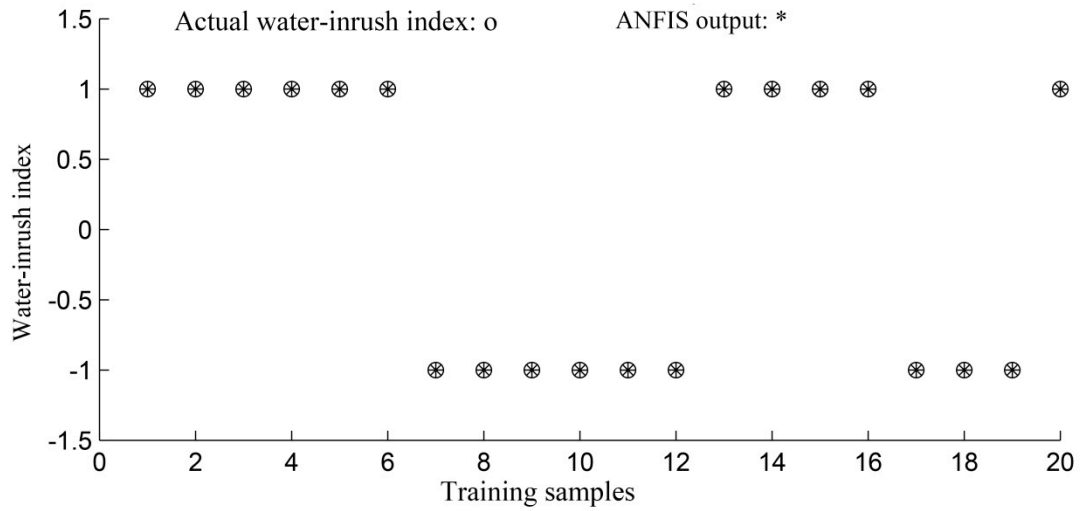

Figure 7. The training results of the ANFIS.

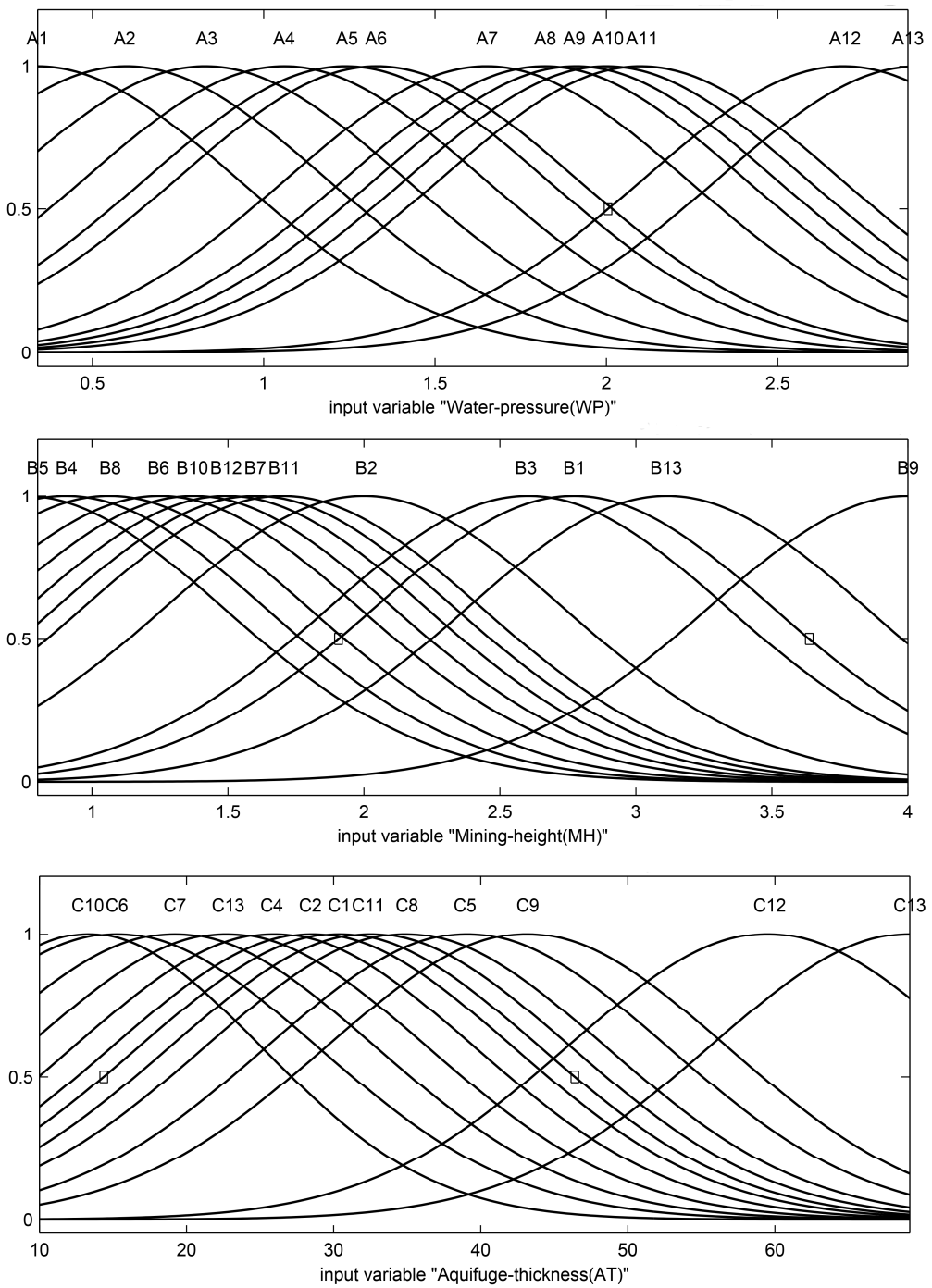

Figure 8. The shape of the membership functions after training (for parameters WP, MH and AT).

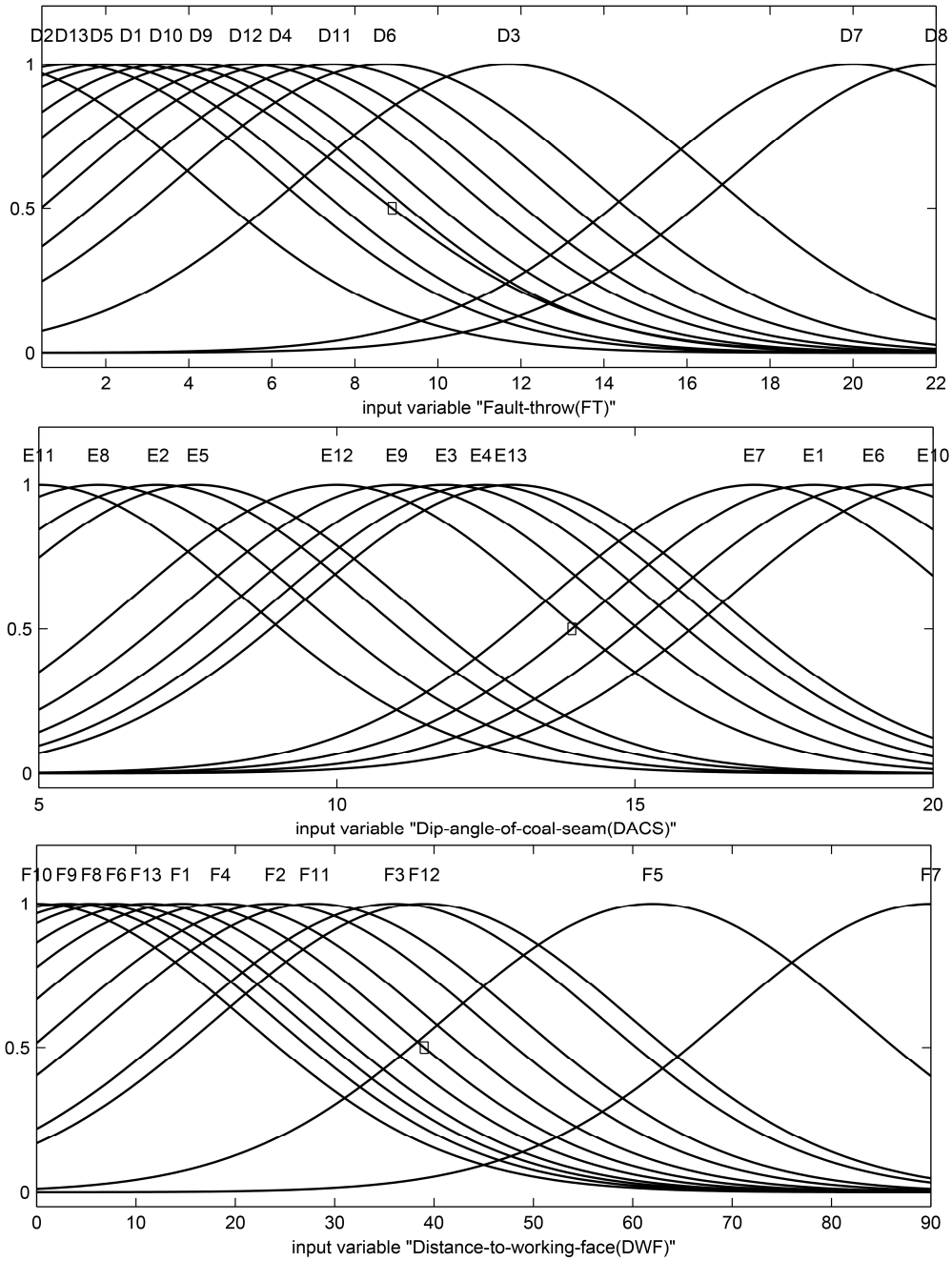

Figure 9. The shape of the membership functions after training (for parameters FT, DACS and DWF).

4.2. Results and Remarks

Actually, the training process of ANFIS is the process of learning knowledge from training samples. Without doubt, the randomly generated initial FIS rules cannot be used to accurately infer the outputs from the sample inputs, but through sample training, the ANFIS can constantly learn knowledge from training samples, modify the membership functions' shape and thus gradually adjust the initial FIS rules. Therefore, the trained FIS rules are the optimized rules corresponding to the input–output pairs of the training samples.

With all the trained FIS rules, which imply all the knowledge learned from the training samples, fuzzy reasoning can thereby be conducted by using these FIS rules to predict the water inrush indexes for any new samples. In Table 2, geological data for another five working faces of different mines

are given, and by means of the 13 trained FIS rules (Figure 6B) we can obtain the reasoning results of the water inrush indexes corresponding to these five working faces (see Table 3). In Figure 10, the reasoning process of the 31,503 working face in Huatai coal mine is displayed (we do not display all of these five cases because their reasoning processes are similar). As can be seen from Figure 10, the water inrush index (0.661) obtained by FIS rules reasoning is neither equal to 1 nor equal to -1; this raises the question of how to evaluate the risk of water inrush by using the obtained water inrush index; in this study, we propose using the method of membership function to solve this problem and more details about this method will be given in the next paragraph.

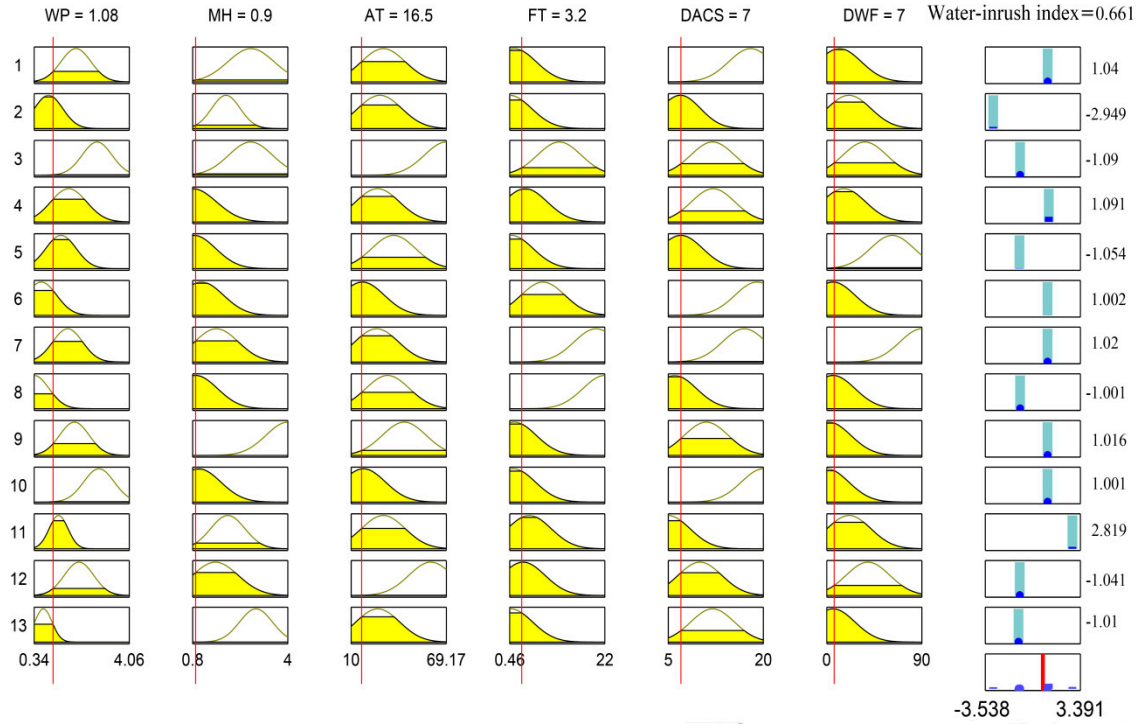

Figure 10. The inferring process of the water inrush index for the 31,503 working face in Huatai coal mine by using the trained rules and trained membership functions.

In the process of ANFIS training, 1 and -1 were selected as the desired outputs to represent water inrush occurring and not occurring respectively. Therefore, here, 1 and -1 are considered as two of the critical values to establish the membership function of water inrush. The discourse domain of the membership function is $[-3.538, 3.391]$ (see Figure 10) and there are two fuzzy subsets included within the discourse domain: the subset of water inrush occurring (Equation (10)) and the subset of water inrush not occurring (Equation (11)). Now, with the established membership function of water inrush, the probability of water inrush occurring or not occurring for any new samples can then be determined. Now, an example is given to show how to calculate the probability of water inrush occurring or not occurring for a new sample by using the method of membership function. For example, the water inrush index of the 31,503 working face in Huatai coal mine is 0.661, so its grade of membership to the subset of water inrush occurring is $(1 + 0.661)/2 = 0.8305$ and to the subset of water inrush not occurring is $(1 - 0.661)/2 = 0.1695$ (see Figure 11); therefore, for the 31,503 working face in Huatai coal mine, the probability of water inrush occurring is 0.8305 and not occurring is 0.1695.

$$y_1 = \begin{cases} 1 & x \geq 1 \\ \frac{1+x}{2} & -1 < x < 1 \\ 0 & x \leq -1 \end{cases} \quad (10)$$

$$y_2 = \begin{cases} 1 & x \leq -1 \\ \frac{1-x}{2} & -1 < x < 1 \\ 0 & x \geq 1 \end{cases} \quad (11)$$

where y_1 represents the membership function of water inrush occurring; y_2 represents the membership function of water inrush not occurring; x denotes the water inrush index inferred by the trained rules.

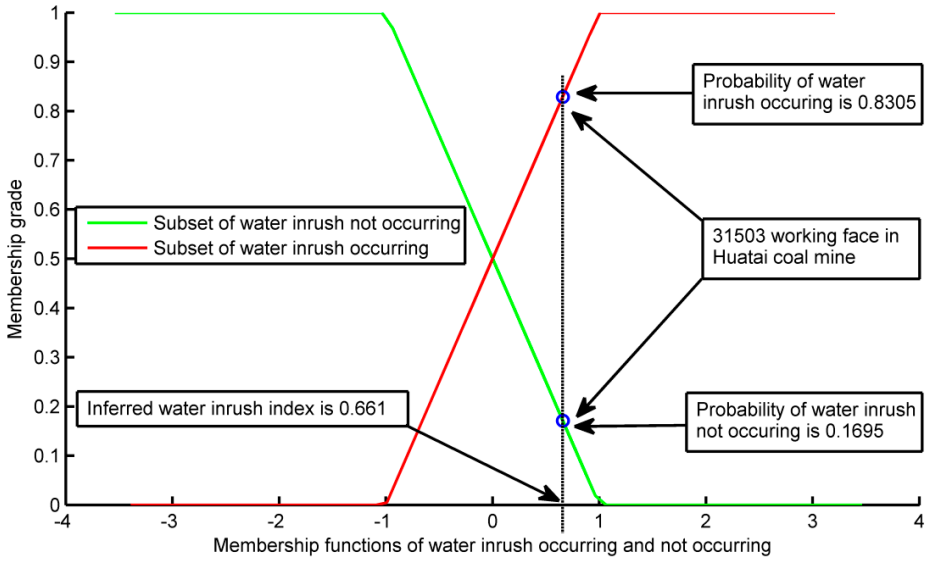

Figure 11. Membership functions of water inrush occurring and not occurring; how to use the water inrush index to obtain the probabilities of water inrush occurring or not occurring is also displayed in this figure.

Using the method of membership function, the predicted results of the five cases corresponding to Table 2 are calculated (as can be seen in Table 3). Our predicted results indicate that there are three working faces for which the probability of occurrence of water inrush is higher than the probability of non-occurrence. The three working faces are the 31,503 working face in Huatai coal mine, the 51,302 working face in Liangzhuang coal mine and the 9602 working face in Baizhuang coal mine; according to Shi's reports [43], water inrush accidents have actually occurred in these three working faces which indicates that our prediction results are consistent with the actual situation.

Table 2. Geological data of the five working faces used for prediction.

Working Faces	(WP)/MPa	(MH)/m	(AT)/m	(FT)/m	(DACS)/°	(DWF)/m
31,503 working face in Huatai coal mine	1.08	0.90	16.50	3.2	7	7
51,302 working face in Liangzhuang coal mine	1.10	1.60	20.00	15.0	11	16
6194 working face in Panxi coal mine	4.06	2.75	65.86	10.0	10	11
9602 working face in Baizhuang coal mine	3.11	2.61	44.30	3.5	11	12
61,106 working face in Huahen coal mine	2.70	2.55	66.97	16.0	12	31

Table 3. Prediction results of the five tested working faces.

Working Faces	Water Inrush Index Obtained by FIS Reasoning	Probability of Water Inrush Occurring	Probability of Water Inrush Not Occurring	Whether Water Inrush Occurred in Actual Situation	Whether the Prediction Is Consistent with the Actual Situation
31,503 working face in Huatai coal mine	0.661	0.8305	0.1695	Yes	Yes
51,302 working face in Liangzhuang coal mine	0.658	0.829	0.171	Yes	Yes
6194 working face in Panxi coal mine	−0.999	0.0005	0.9995	No	Yes
9602 working face in Baizhuang coal mine	0.122	0.561	0.439	Yes	Yes
61,106 working face in Huahen coal mine	−1	0	1	No	Yes

5. Conclusions

The aim of this paper was to develop a more advanced method for the assessment of mine water inrushes, and to reduce the occurrence of a large number of ongoing water inrush accidents in developing countries. In this paper, the technique of the ANFIS was used to predict the probability of the fault-induced water inrush being developed. All the main parameters related to the hydraulic properties of the aquifer, the water-resisting properties of the aquifuge and the mining-induced stresses were considered in the developed method. With these main parameters, an ANFIS model was constructed and the subtractive clustering method was used to generate the initial FIS rules. In the training step, twenty real water inrush cases were used to train the initial rules and the membership functions.

The advantage of the ANFIS is that after the training process, the trained FIS rules and the modified membership functions imply all the knowledge learned from the training samples. With the other five water inrush cases selected from different mines, we predicted their water inrush probabilities by using the trained FIS rules and the method of membership function. The final prediction results were consistent with the actual situation.

It needs to be emphasized here that, in the current study, only six main parameters were considered to assess the risk of water inrush. Certainly, there are some improvements compared to the traditional approach of considering only two parameters (the groundwater pressure and the aquifuge thickness) but, in order to predict the fault-induced water inrush in a more efficient way, more parameters could be considered, such as mining depth; mining method; mining intensity; working face length; or strength of the floor, to name but a few. This can be the subject of a future study.

Acknowledgments: The authors would like to thank The China Scholarship Council (CSC) for financial supports.

Author Contributions: This paper was written by Qinlong Zhou, Juan Herrera-Herbert contributed to reviewing and editing the manuscript, Arturo Hidalgo contributed to improving and designing the ANFIS modeling and training.

Conflicts of Interest: The authors declare no conflict of interest.

References

1. Bringemier, D. Inrush and mine inundation—A real threat to Australian coal mines. In Proceedings of the International Mine Water Association Annual Conference, Bunbury, Australia, 30 September–4 October 2012.
2. Przemysław, B. Water hazard assessment in active shafts in Upper Silesian Coal Basin Mines. *Mine Water Environ.* **2011**, *30*, 302–311.
3. Zhang, J.C. Investigations of water inrushes from aquifers under coal seams. *Int. J. Rock Mech. Min. Sci.* **2005**, *42*, 350–360. [CrossRef]
4. Wang, Y.; Yang, W.F.; Li, M.; Liu, X. Risk assessment of floor water inrush in coal mines based on secondary fuzzy comprehensive evaluation. *Int. J. Rock Mech. Min. Sci.* **2012**, *52*, 50–55. [CrossRef]
5. Meng, Z.P.; Li, G.; Xie, X.T. A geological assessment method of floor water inrush risk and its application. *Eng. Geol.* **2012**, *143–144*, 51–60. [CrossRef]
6. Edincliler, A.; Cabalar, A.F.; Cevik, A. Modelling dynamic behaviour of sand–waste tires mixtures using Neural Networks and Neuro-Fuzzy. *Eur. J. Environ. Civ. Eng.* **2013**, *17*, 720–741. [CrossRef]
7. Dieu, T.B.; Biswajeet, P.; Owe, L.; Inge, R.; Oystein, B.D. Landslide susceptibility mapping at Hoa Binh province (Vietnam) using an adaptive neuro-fuzzy inference system and GIS. *Comput. Geosci.* **2012**, *45*, 199–211.
8. Szymczyk, P.; Szymczyk, M. Classification of geological structure using ground penetrating radar and Laplace transform artificial neural networks. *Neurocomputing* **2005**, *148*, 354–362. [CrossRef]
9. Edincliler, A.; Cabalar, A.F.; Cagatay, A.; Cevik, A. Triaxial compression behavior of sand and tire wastes using neural networks. *Neural Comput. Appl.* **2012**, *21*, 441–452. [CrossRef]
10. Alemdag, S.; Gurocak, Z.; Cevik, A.; Cabalar, A.F.; Gokceoglu, C. Modeling deformation modulus of a stratified sedimentary rock mass using neural network, fuzzy inference and genetic programming. *Eng. Geol.* **2016**, *203*, 70–82. [CrossRef]

11. Inhye, P.; Jaewon, C.; Moung, J.L.; Saro, L. Application of an adaptive neuro-fuzzy inference system to ground subsidence hazard mapping. *Comput. Geosci.* **2012**, *48*, 228–238.
12. Yilmaz, I.; Kaynar, O. Multiple regression, ANN (RBF, MLP) and ANFIS models for prediction of swell potential of clayey soils. *Expert Syst. Appl.* **2011**, *38*, 5958–5966. [CrossRef]
13. Cevik, A.; Sezer, E.A.; Cabalar, A.F.; Gokceoglu, C. Modeling of the uniaxial compressive strength of some clay-bearing rocks using neural network. *Appl. Soft Comput.* **2011**, *11*, 2587–2594. [CrossRef]
14. Singh, R.; Kainthola, A.; Singh, T.N. Estimation of elastic constant of rocks using an ANFIS approach. *Appl. Soft Comput.* **2012**, *12*, 40–45. [CrossRef]
15. Bedri, K.; Nicolas, F. Hydraulic head interpolation using ANFIS—Model selection and sensitivity analysis. *Comput. Geosci.* **2012**, *38*, 43–51.
16. Shahin, M.A.; Maier, H.R.; Jaksa, M.B. Settlement prediction of shallow foundations on granular soils using B-spline neurofuzzy models. *Comput. Geotech.* **2003**, *30*, 637–647. [CrossRef]
17. Cabalar, A.F.; Cevik, A.; Gokceoglu, C.; Baykal, G. Neuro-fuzzy based constitutive modeling of undrained response of Leighton Buzzard Sand mixtures. *Expert Syst. Appl.* **2010**, *37*, 842–851. [CrossRef]
18. Cabalar, A.F.; Cevik, A.; Guzelbey, I.H. Constitutive modeling of Leighton Buzzard Sands using genetic programming. *Neural Comput. Appl.* **2010**, *19*, 657–665. [CrossRef]
19. Cabalar, A.F.; Cevik, A. Modelling damping ratio and shear modulus of sand–mica mixtures using neural networks. *Eng. Geol.* **2009**, *104*, 31–40. [CrossRef]
20. Wu, Q.; Xu, H.; Pang, W. GIS and ANN coupling model: An innovative approach to evaluate vulnerability of karst water inrush in coalmines of north China. *Environ. Geol.* **2008**, *54*, 937–943. [CrossRef]
21. Sian, L.; Victor, B.; Jenni, T. Fault architecture and deformation processes within poorly lithified rift Sediments, Central Greece. *J. Struct. Geol.* **2011**, *33*, 1554–1568.
22. Caine, J.S.; Evans, J.P.; Forster, C.B. Fault zone architecture and permeability structure. *Geology* **1996**, *24*, 1025–1028. [CrossRef]
23. Gudmundsson, A.; Simmenes, T.H.; Larsen, B.; Philipp, S.L. Effects of internal structure and local stresses on fracture propagation, deflection, and arrest in fault zones. *J. Struct. Geol.* **2010**, *32*, 1643–1655. [CrossRef]
24. Rawling, G.C.; Goodwin, L.B.; Wilson, J.L. Internal architecture, permeability structure, and hydrologic significance of contrasting fault-zone types. *Geology* **2011**, *29*, 43–46. [CrossRef]
25. Bense, V.F.; Van Balen, R.T. Hydrogeological aspects of fault zones on various scales in the Roer Valley Rift System. *J. Geochem. Explor.* **2003**, *78–79*, 317–320. [CrossRef]
26. Goddard, J.V.; Evans, J.P. Chemical changes and fluid-rock interaction in faults of crystalline thrust sheets, northwestern Wyoming, USA. *J. Struct. Geol.* **1995**, *17*, 533–547. [CrossRef]
27. Sameh, W.A.M.; Broder, J.M. Interpretation of Groundwater Flow into Fractured Aquifer. *Int. J. Geosci.* **2012**, *3*, 357–364.
28. Palchik, V. Formation of fractured zones in overburden due to longwall mining. *Environ. Geol.* **2003**, *41*, 28–38.
29. Liang, D.X.; Jiang, Z.Q.; Guan, Y.Z. Field research: Measuring water pressure resistance in a fault-induced fracture zone. *Mine Water Environ.* **2015**, *34*, 320–328. [CrossRef]
30. Jonny, R.; Antonio, P.R.; Frederic, C.; George, J.M. Modeling of fault activation and seismicity by injection directly into a fault zone associated with hydraulic fracturing of shale-gas reservoirs. *J. Petrol. Sci. Eng.* **2015**, *127*, 377–386.
31. IsIam, M.R.; Ryuichi, S. Mining-induced fault reactivation associated with the main conveyor belt roadway and safety of the Barapukuria Coal Mine in Bangladesh: Constraints from BEM simulations. *Int. J. Coal Geol.* **2009**, *79*, 115–130.
32. Li, J.; Xu, Y.; Xie, X.; Yao, Y.; Gao, Y. Influence of mining height on coal seam floor failure depth. *J. China Coal Soc.* **2015**, *40*, 303–310. (In Chinese).
33. Miao, X.; Cui, X.; Wang, J.; Xu, J. The height of fractured water-conducting zone in undermined rock strata. *Eng. Geol.* **2011**, *120*, 32–39. [CrossRef]
34. Zadeh, L.A. Fuzzy sets as a basis for a theory of possibility. *Fuzzy Sets Syst.* **1978**, *1*, 3–28. [CrossRef]
35. Fukushima, K.; Miyake, S.; Ito, T. Neocognitron: A neural network model for a mechanism of visual pattern recognition. *IEEE Trans. Syst. Man Cybern.* **1983**, *5*, 826–834. [CrossRef]
36. Mcculloch, W.S.; Pitts, W. A logical calculus of the ideas immanent in nervous activity. *Bull. Math. Biol.* **1943**, *5*, 115–133. [CrossRef]

37. Jang, J.S.R. Input selection for ANFIS learning. In Proceedings of the Fifth IEEE International Conference on Fuzzy Systems, New Orleans, LA, USA, 8–11 September 1996; Volume 3, pp. 1493–1499.
38. Jang, J.S.R. Fuzzy modeling using generalized neural networks and Kalman filter algorithm. In Proceedings of the Ninth National Conference on Artificial Intelligence, Anaheim, CA, USA, 14–19 July 1991; Volume 2, pp. 762–767.
39. Takagi, T.; Sugeno, M. Fuzzy identification of systems and its applications to modeling and control. *IEEE Trans. Syst. Man. Cybern.* **1985**, *15*, 116–132. [CrossRef]
40. Mamdani, E.H.; Assilian, S. An experiment in linguistic synthesis with a fuzzy logic controller. *Int. J. Man Mach. Stud.* **1999**, *51*, 135–147. [CrossRef]
41. Larsen, P. Industrial applications of fuzzy-logic control. *Int. J. Man Mach. Stud.* **1980**, *12*, 3–10. [CrossRef]
42. Jang, J.S.R. Anfis: Adaptive-network-based fuzzy inference system. *IEEE Trans. Syst. Man. Cybern.* **1993**, *23*, 665–685. [CrossRef]
43. Shi, L.Q.; Tan, X.P.; Wang, J.; Ji, X.K.; Niu, C.; Xu, D.J. Risk assessment of water inrush based on PCA_Fuzzy_PSO_SVC. *J. China Coal Soc.* **2015**, *40*, 167–171. (In Chinese).
44. Chiu, S.L. Fuzzy model identification based on cluster estimation. *J. Intell. Fuzzy Syst.* **1994**, *2*, 267–278.
45. Chiu, S.L. An efficient method for extracting fuzzy classification rules from high dimensional data. *J. Adv. Comput. Intell.* **1997**, *1*, 1–7.